

BOND BEHAVIOR OF TEXTILE REINFORCED FINE-GRAINED ALKALI ACTIVATED CEMENT CONCRETE

Biruk Hailu Tekle, Federation University, Australia, b.tekle@federation.edu.au

Dennis Messerer, Leipzig University of Applied Sciences, Germany, d.messerer@htwk-leipzig.de

Klaus Holschemacher, Leipzig University of Applied Sciences, Germany, k.holschemacher@htwk-leipzig.de

Amar Khennane, UNSW Canberra, Australia, a.khennane@adfa.edu.au

ABSTRACT

This study investigates the bond behavior of textile-reinforced alkali activated cement (AAC) concrete. AAC is a promising substitute for ordinary Portland cement, addressing the environmental concerns associated with the latter. Textile reinforcements are made of high-performance materials such as carbon. Using fiber-reinforced polymer (FRP) textiles with AAC concrete makes it possible to have corrosion-resistant, environmentally friendly thin concrete structures. This study investigates the bond between FRP textiles and fine-grained AAC concrete. The effect of concrete casting position, textile orientation, and concrete strength was investigated. The compressive strength showed a significant influence, while the casting position showed no considerable effect on the bond. Changing the textile orientation showed some change in bond strength.

KEYWORDS

textile-reinforced concrete; alkali activated cement; pullout failure; bond; fine-grained concrete

INTRODUCTION

In recent years textile reinforced concrete (TRC) has found momentum in the construction industry (Halvaei et al., 2020; Holschemacher, 2020). TRC enables the production of thin structural and non-structural components while avoiding the negative effects of corrosion. Typically, this composite material consists of a cement-based matrix with fine-grained properties and reinforced with fiber-reinforced polymer (FRP) elements. TRC exhibits notable characteristics such as high tensile strength, excellent deformation tolerance, and superior durability, primarily due to its non-metallic reinforcement (Mechtcherine et al., 2016). However, the increasing demand for ordinary Portland cement (OPC) binders in high-performance concretes has impacted negatively the CO₂ balance. As a result, ongoing investigations are focused on replacing OPC binders with alternative matrices that are more environmentally friendly and corrosion-resistant, such as alkali activated cement (AAC). While the material behavior of TRC with conventional OPC binders has been studied to some extent, material properties for the combination of FRP reinforcements with AAC are mainly lacking in the literature. Existing investigations usually deal with the flexural and tensile load-bearing capacity of AAC-based TRC (Le Chi & Louda, 2019; Le Chi et al., 2018). Parameters, such as the bond behavior, are hardly available. Bond is one of the main indicators for the overall load-bearing and deformation behavior of thin-walled components made of TRC. This paper, therefore, presents an experimental study of pullout test to understand the bond behavior of textile reinforced AAC concrete.

EXPERIMENTAL PROGRAM

Materials

Fly ash (FA), ground granulated blast furnace slag (GGBS), and silica fume (SF) were used in the preparation of the AAC concretes. The FA, GGBS, and SF comply with EN 450-1, EN 15167-1, and EN 13263-1 requirements, respectively. The chemical compositions of these source materials are summarized in Table 1. The activator solution used is a mixture of sodium silicate and sodium hydroxide. The sodium silicate solution includes 26.82% silicate, 8.2% sodium oxide, and 64.98%

water, while the sodium hydroxide is a 50% by weight solution. Furthermore, a fine aggregate with a maximum aggregate size of 4 mm was used. Additional fines (0.1 – 0.35 mm) were also used.

Table 1. Chemical composition of ingredients

Composition	FA (%)	GGBS (%)	SF* (%)
SiO ₂	49.79	34.48	93.81
Al ₂ O ₃	26.71	11.48	0.48
Fe ₂ O ₃	8.57	-	1.49
MgO	2.47	7.08	0.46
CaO	4.34	42.43	0.30
K ₂ O	3.36	0.66	0.77
Na ₂ O	1.28	0.56	0.42
SO ₃	1.49	2.17	0.20
TiO ₂	1.23	1.14	-
Specific surface area (m ² /g)	0.45	0.46	19.40
Specific gravity (g/cm ³)	2.28	2.91	2.20

*manufacturer specification

For this study, a biaxial carbon fiber mesh with epoxy impregnation was used. Figure 1 provides a photograph of the carbon textile grid. The individual fiber strands possess a flat, oval-shaped cross-section, and they are interconnected in orthogonal directions using a double-knitted thread to maintain their position. The cured resin serves to maintain dimensional stability and ensure continuous alignment of the elements. Table 2 presents a summary of the various properties associated with the carbon textile grid.

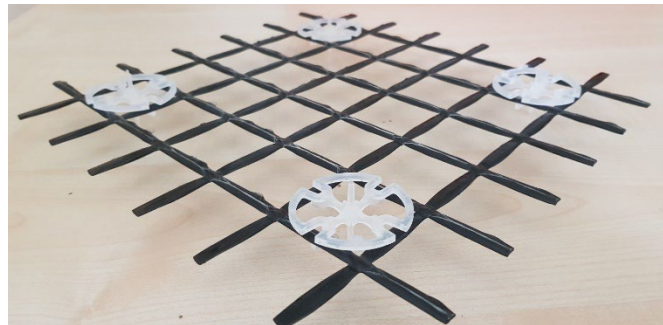


Figure 1: Textile grid

Table 2. Characteristic values of Solidian GRID Q140-CCE-25

Data	Unit	Weft	Warp
Fiber material		Carbon	Carbon
Impregnation material		Epoxy	Epoxy
Center to center distance	mm	25	25
Cross-section area	mm ² /m	142	142
Cross-section of the strand	mm ²	3.62	3.62
Tensile strength	N/mm ²	3100	3300
E-Modulus	N/mm ²	200,000 – 250,000	

Test specimen and testing method

Bond is commonly investigated using pullout tests like the RILEM-RC 6 test method. However, despite being a simple test method, the stress conditions in the specimens are not representative of most of the situations encountered in practice. Due to the support condition, some portion of the specimen is under compression. Hence the test method is mainly used for the comparative analysis of bond between different parameters. Pullout test setups were also used for textile reinforced concrete with some modifications (Krüger, 2004; Tekle, Messerer, et al., 2021). The method Krüger (2004) developed involves a single-layered textile-reinforced concrete specimen with a predefined cracking section. The

cracking is made to give an unsymmetrical bond length below and above the cracking line. The longer section anchors the textile to avoid pullout. The shorter section acts as the test section.

As shown in Figure 2, a modified test setup is used in the present study. No support is used at the bottom of the specimen to avoid compressive stress. Instead, the specimen is clamped at the upper end by 15 mm thick steel plates. Thin elastomers are inserted between the specimen and the steel plates to ensure uniform clamping. A single fiber strand is tested to understand the bond behavior of the sole strand without the influence of the additional weft and warp strands. The influence of the additional strands is taken as a parameter. The fiber strand is pulled out similar to the conventional pullout test. However, to prevent premature failure due to grip, a 2.5 mm thick leather was wrapped around the fiber strand according to the recommendation of Wendler et al. (2020). The force was measured using a load cell with a load capacity of 20 kN. Two linear variable displacement transducers (LVDT) were attached at the free-end and loaded end of the fiber strand to monitor the slips. The test was displacement-controlled at a 1 mm/min speed.

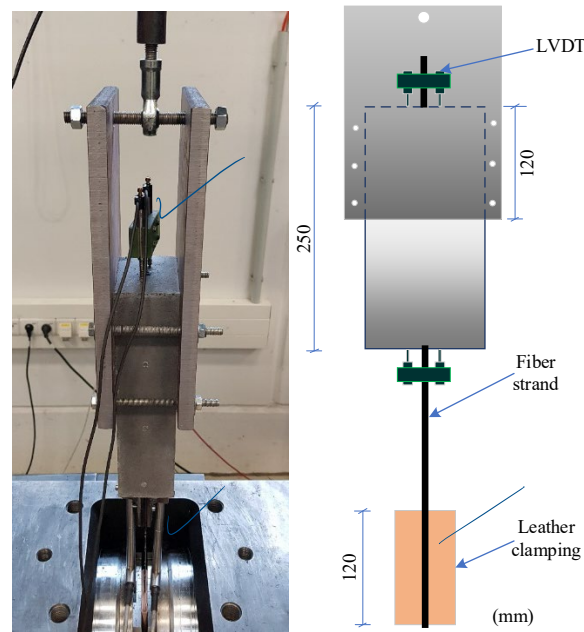


Figure 2: Test specimen setup

Further details of the specimen are shown in Figure 3. The thickness of the specimen is 60 mm, thicker than commonly used TRC members to avoid splitting failure. Figure 3b is used as one parameter investigating the influence of the transverse textile reinforcements on the bond. The desired embedment length is achieved by putting PVC tubes (Figure 3a) or cutting the fiber strand at the desired location (Figure 3b). A bond length of 25 mm was used. This length corresponds to the mesh spacing.

Investigated parameters

The experimental program aimed to evaluate the bond performance and the effect of different parameters on the bond behavior of textiles reinforced fine grained AAC concrete. The influence of concrete strength, casting direction, and textile reinforcement direction is investigated. Three concrete mixtures were taken as a parameter, C1, C2, and C3 as shown in Table 3. These concretes were designed for different compressive strengths to investigate the effect of concrete strength. The mix proportions with their respective compressive strength are shown in Table 3. Further details on the development of the fine grained AAC concrete are available from previous works of the authors (Tekle, Hertwig, et al., 2021a, 2021b; Tekle & Holschemacher, 2022).

The fiber strand direction was taken as a parameter. In the control specimen, the major axis of the strand's ellipse was aligned with the width of the specimen. In the experimental specimen, it is aligned

with the thickness of the specimen (Figure 3c). Two casting directions (Figure 3d), casting parallel and perpendicular to the tested fiber strand, are taken as parameters. The specimens are identified by the concrete type (C1, C2, and C3), the direction of casting (C2CD), the presence of transverse reinforcement (C2T), the direction of the fiber strand (C2SD), and the specimen number.

Table 3. Concrete mix compositions

Ingredients (kg/m ³)	C1	C2	C3
Sand 2-4 mm	448	472	488
Sand 0-2 mm	560	590	610
Fines 0.1-0.35 mm	112	118	122
FA	302.5	357.5	412.5
GGBS	220	260	300
SF	27.5	32.5	37.5
SHL	56	66	76
SSL	140	165	191
Water	200	113	33
Superplasticizer	-	30	51
Na ₂ O/SiO ₂ ^a	0.13	0.13	0.13
SiO ₂ /Al ₂ O ₃ ^a	4.63	4.63	4.63
H ₂ O/Na ₂ O ^a	29.17	19.82	13.43
Compressive strength (MPa)	29	64	79

SHL, and SSL solutions of sodium hydroxide and sodium silicate.

^a Molar ratio of mixtures (including activators, binders, and additional water).

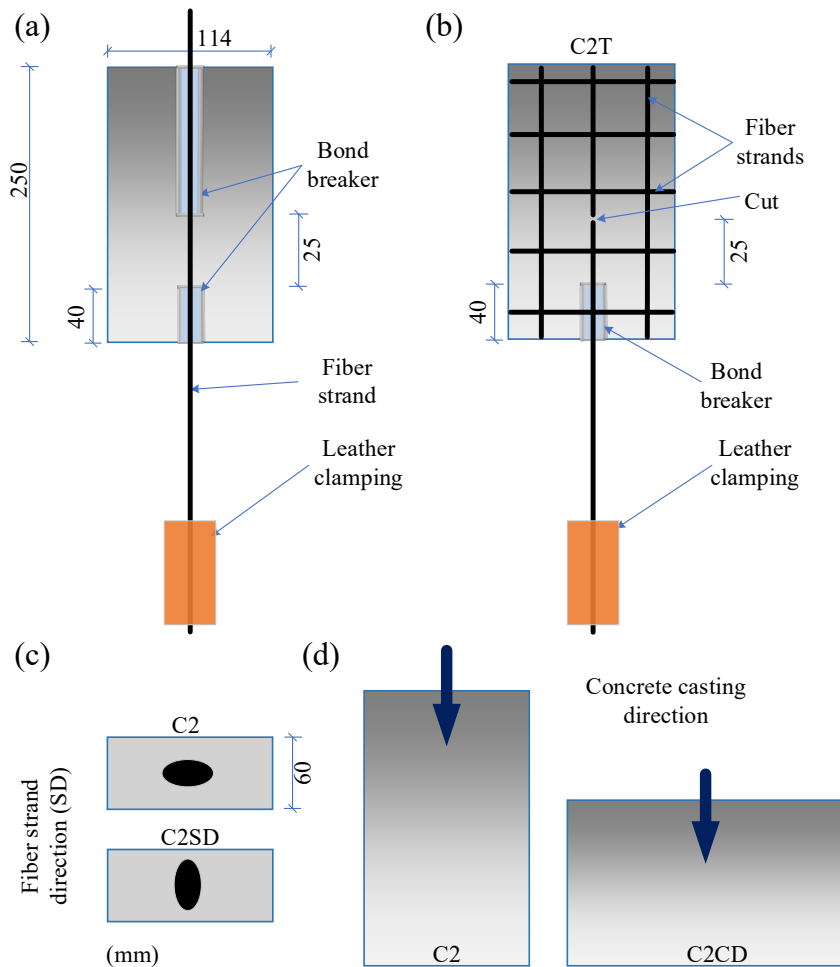


Figure 3: Bond test specimen details

RESULTS AND DISCUSSIONS

Results

Table 4 shows the pullout load, free-end and loaded-end slips, and the failure mode of the specimens. The average bond stress cannot be calculated because the fiber strand does not have a constant cross-section along the embedment length. Hence the analyses were done based on the average pullout forces.

Table 4. Test results

Specimen Name	Average failure load (kN)	Free-end slip (mm)	Loaded-end slip (mm)	Failure mode
C1-1	2.5	4.8	5.0	Pullout
C1-2	2.4	3.2	3.2	Pullout
C1-3	3.1	4.3	4.4	Pullout
C2-1	4.8	8.3	8.7	Pullout
C2-2	5.5	6.0	6.5	Pullout
C2-3	5.3	6.7	7.1	Pullout
C3-1	5.8	6.8	7.2	Pullout
C3-2	5.9	6.0	6.4	Pullout
C2T-1	5.2	NA	7.4	Pullout
C2T-2	5.6	NA	8.7	Pullout
C2T-3	4.8	NA	8.9	Pullout
C2CD-1	5.6	5.8	6.0	Pullout ^a
C2CD-2	4.6	10.2	12.7	Pullout
C2SD-1	4.5	10.7	11.9	Pullout
C2SD-2	4.4	10.1	10.6	Pullout
C2SD-3	5.1	8.8	9.2	Splitting

a: transverse cracking was also observed. NA: test results not available

Failure mode

In all specimens except for series C2SD-3, failure was due to the pullout of the textile. After the pullout failure, the fiber strands were pulled entirely out until the embedded portion of the fiber strand was visible to investigate the interface surfaces of the concrete and the textile. The additional pullout force applied to pull the fiber strands entirely out after the peak load resulted in concrete splitting. Investigation of the embedded portion showed minor damage on the surfaces of the fiber strand. The concrete surface was also mostly intact.

Splitting failure (before the peak load) was observed only in the case of specimen C2SD-3. However, even in this specimen, the splitting happened after a significant free-end slip of about 8.8 mm. For all the other specimens, splitting only occurred during the post-peak pulling of the fiber strand. The post-peak splitting is because of the introduction of a new undamaged fiber strand section into the bond length resulting in a higher mechanical interlock induced splitting stress. The pre-peak and post-peak splitting were along the textile layer (major ellipse dimension). In the case of C2SD; the specimens with rotated fiber strands, the direction of the splitting crack changed with the direction of the major ellipse axis (Figure 4).



Figure 4: Concrete failure mode

Force-slip relationships

Figure 5 shows the force-slip relationship for the different specimens. The curves present a high initial stiffness caused by the undisturbed adhesion and mechanical interlock between the fiber strand and the concrete. Once this adhesion is lost, the stiffness reduces gradually until flattening and reaching the maximum pullout load. After the peak, the load drops either gradually with the increase of the slip in case of pullout failure or suddenly in case of splitting failure.

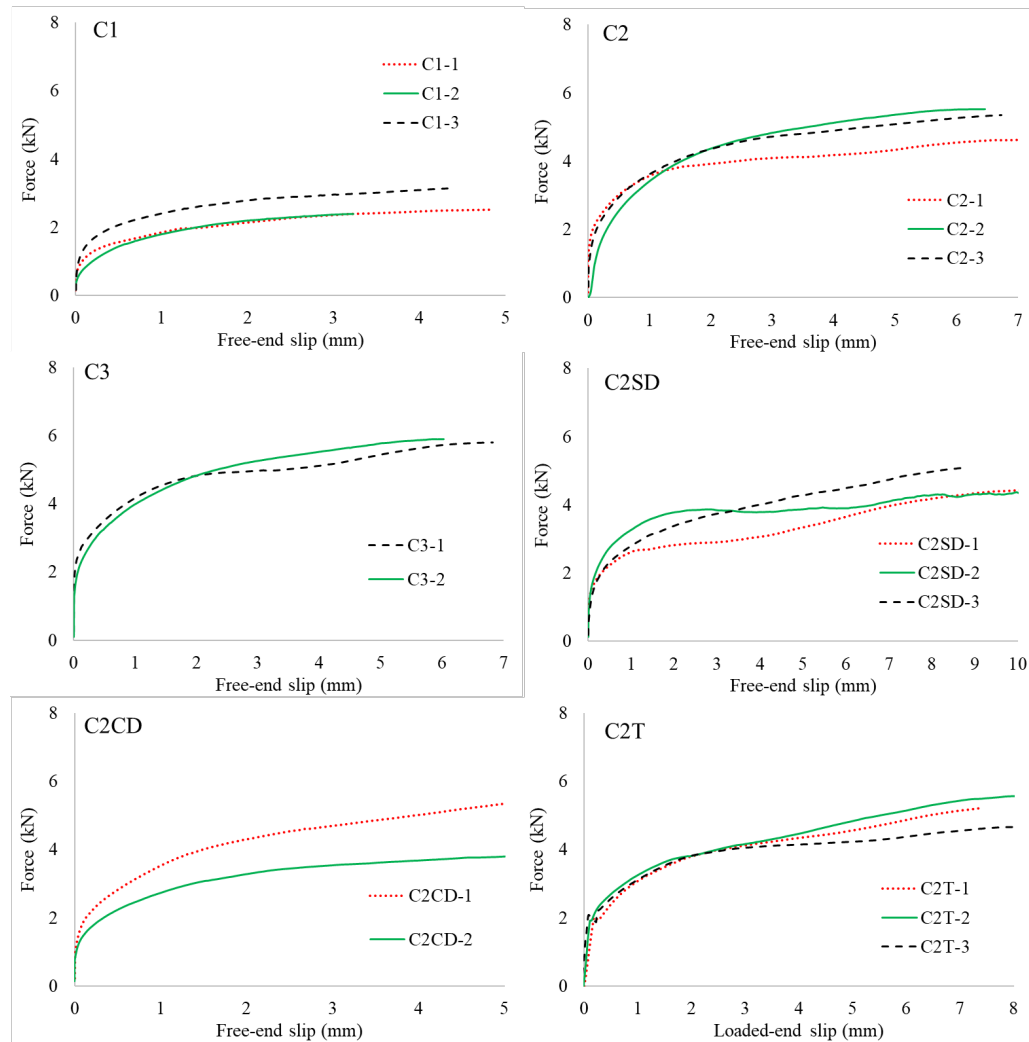


Figure 5: Load-slip curves (no free end slip available for C2T specimens)

Effect of parameters

Transverse fibre strand

The specimens with transverse reinforcements (C2T) showed a sudden load drop at about 2 kN (Figure 5). This is due to the detaching of the knitted transverse strands from the tested strand. This connection is only for stability during installation. These specimens also showed hardening of the force-slip curve starting at about 3 mm slip. This is believed to be due to the interaction of the transverse and longitudinal fiber strands. The cross-sections of the fibers are minimum at the intersection between the transverse and longitudinal fiber strands. As the load increases, the longitudinal strand slides against the transverse one. Due to the increase in the minor ellipse dimension of the longitudinal strand (cross-sectional dimensions increase from the intersection to the mid-section), a higher force is required to pull the strand resulting in the observed hardening.

The presence of the transverse fiber strands within the bond length resulted in no significant change in the peak bond force values. This confirms that bond study for textile reinforcements can be effectively performed using single fiber strands. Such a study on a single fiber strand can give important results as

to the bond behavior of the single fiber strand. This can be an important input for numerical modeling works.

Concrete strength

Three concrete strengths were tested. The lower compressive strength specimens (C1) showed lower pullout forces and slips than C2 and C3. Xu and Li (2007) also observed similar results for OPC concrete reinforced with textile reinforcements. The higher the concrete strength, the higher the concrete's resistance to the textile's pullout. An equation was obtained for the pullout force in relation to the compressive strength using least square optimization. As shown in Figure 6, the pullout force is proportional to the concrete strength to the power of $\frac{3}{4}$. For conventional steel reinforced concrete structures, bond is commonly normalized with respect to the square root of the compressive strength (ACI 408-03, 2012). However, other relations have also been observed based on factors such as the extent of the compressive strength and the presence of confinement (Azizinamini et al., 1995; Jun & David).

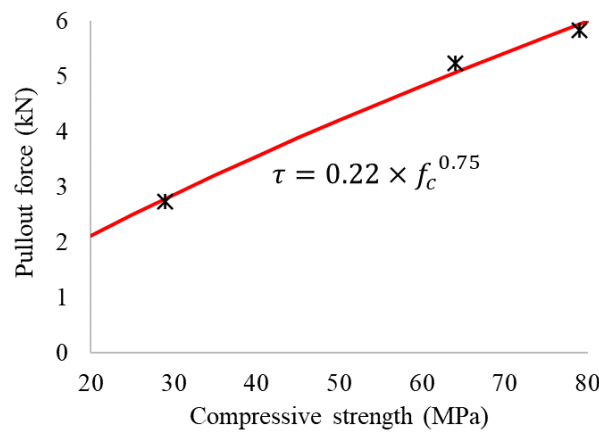


Figure 6: Influence of compressive strength on bond strength

Casting direction

The effect of casting direction on the bond force is investigated by casting the concrete along and perpendicular to the textile reinforcement, as shown in Figure 3. As can be observed from Table 4, no significant effect was observed. The effect of casting position gets pronounced with the amount of bleed water that accumulates under the reinforcement, which in turn depends on the size of the reinforcement (Tekle, Messerer, et al., 2021). In the current study, the amount of bleed water that can accumulate under the textile reinforcement is minimal as the size of the fiber strand is small. Hence casting direction has no major effect.

Textile direction

In C2SD, the fiber strand direction was changed; the major ellipse direction of the strand was aligned with the thickness of the concrete (Figure 3c). This resulted in some reduction of the pullout force, as can be observed in Table 4. The concrete cover along the major ellipse direction decreased as the strand was rotated (the concrete specimen's size along the strand's major axis changed from 114 mm to 60 mm as the strand rotated), causing less confinement. This resulted in the observed lower pullout force.

CONCLUSIONS

This study focused on examining the bond behavior of carbon textile reinforced alkali activated cement (AAC). To prevent internal compressive stresses and premature splitting of the concrete, a modified test setup was developed. The investigated parameters included concrete strength, the presence of transverse textile strands, concrete casting direction, and the orientation of the fiber strands. The evaluation of the tests revealed the following findings:

- The presence of transverse fiber strands did not have a significant effect on the maximum bond force. This suggests that the bond characteristics of textile reinforcements can be effectively studied using single fiber strands.
- An increase in compressive strength resulted in an increase in the pullout bond force. The relationship between the pullout force and concrete strength followed a proportional trend with the concrete strength raised to the power of $\frac{3}{4}$.
- The casting direction did not show a significant impact on the pullout force. However, a change in the textile direction did affect the pullout force due to the alteration in the concrete cover.

These results contribute to our understanding of the bond behavior between carbon textile reinforcements and AAC, providing insights into the influence of different parameters on the pullout force.

ACKNOWLEDGEMENT

The authors gratefully acknowledge the financial support of the Alexander von Humboldt Foundation (1206836-AUS-HFST-P).

CONFLICT OF INTEREST

The authors declare that they have no conflicts of interest associated with the work presented in this paper.

DATA AVAILABILITY

Data on which this paper is based is available from the authors upon reasonable request.

REFERENCES

- ACI 408-03. (2012). Bond and Development of Straight Reinforcing Bars in Tension. In. Farmington Hills, Mich.: American Concrete Institute.
- Azizinamini, A., Chisala, M., & Ghosh, S. K. (1995). Tension development length of reinforcing bars embedded in high-strength concrete. *Engineering Structures*, 17(7), 512-522. [https://doi.org/https://doi.org/10.1016/0141-0296\(95\)00096-P](https://doi.org/https://doi.org/10.1016/0141-0296(95)00096-P)
- EN 450-1. (2012). Fly ash for concrete - Part 1: Definition, specifications and conformity criteria. In. Brussels: CEN.
- EN 13263-1. (2005). Silica fume for concrete - Part 1: Definitions, requirements and conformity criteria.
- EN 15167-1. (2006). Ground granulated blast furnace slag for use in concrete, mortar and grout - Part 1: Definitions, specifications and conformity criteria. In. Brussels: CEN.
- Halvaei, M., Jamshidi, M., Latifi, M., & Ejtemaei, M. (2020). Experimental investigation and modelling of flexural properties of carbon textile reinforced concrete. *Construction and Building Materials*, 262, 120877. <https://doi.org/10.1016/j.conbuildmat.2020.120877>
- Holschemacher, K. (2020). Application of Textile Reinforced Concrete in Precast Concrete Industry. *IOP Conference Series: Materials Science and Engineering*, 753, 042086. <https://doi.org/10.1088/1757-899x/753/4/042086>
- Jun, Z., & David, D. Splice Strength of Conventional and High Relative Rib Area Bars in Normal and High-Strength Concrete. *ACI Structural Journal*, 97(4). <https://doi.org/10.14359/7428>
- Krüger, M. (2004). *Vorgespannter textildbewehrter Beton: Prestressed textile-reinforced concrete* [Universität Stuttgart]. Stuttgart, Germany.
- Le Chi, H., & Louda, P. (2019). Experimental Investigation of Four-Point Flexural Behavior of Textile Reinforcement in Geopolymer Mortar. *International Journal of Engineering and Technology*.
- Le Chi, H., Louda, P., Periyasamy, A. P., Bakalova, T., & Kovacic, V. (2018). Flexural Behavior of Carbon Textile-Reinforced Geopolymer Composite Thin Plate. *Fibers*, 6(4), 87. <https://www.mdpi.com/2079-6439/6/4/87>
- Mechtcherine, V., Schneider, K., & Brameshuber, W. (Eds.). (2016). *Mineral-based matrices for textile-reinforced concrete*. Woodhead Publishing.

- RILEM RC 6. (1994). Recommendations for the Testing and Use of Constructions Materials: RC 6 Bond test for reinforcement steel. Pull-out test. In: E & FN SPON.
- Tekle, B. H., Hertwig, L., & Holschemacher, K. (2021a). Rheology of Alkali-Activated Blended Binder Mixtures. *Materials*, 14(18), 5405. <https://www.mdpi.com/1996-1944/14/18/5405>
- Tekle, B. H., Hertwig, L., & Holschemacher, K. (2021b). Setting Time and Strength Monitoring of Alkali-Activated Cement Mixtures by Ultrasonic Testing. *Materials*, 14(8), 1889. <https://www.mdpi.com/1996-1944/14/8/1889>
- Tekle, B. H., & Holschemacher, K. (2022). Alkali activated cement mixture at ambient curing: Strength, workability, and setting time. *Structural Concrete*, 23(4), 2496-2509. <https://doi.org/https://doi.org/10.1002/suco.202100274>
- Tekle, B. H., Messerer, D., & Holschemacher, K. (2021). Bond induced concrete splitting failure in textile-reinforced fine-grained concrete. *Construction and Building Materials*, 303, 124503. <https://doi.org/10.1016/j.conbuildmat.2021.124503>
- Wendler, J., Hahn, L., Farwig, K., Nocke, A., Scheerer, S., Curbach, M., & Cherif, C. (2020). Entwicklung eines neuartigen Prüfverfahrens zur Untersuchung der Zugfestigkeit von Fasersträngen für textile Bewehrungsstrukturen: Development of a new test method to investigate the tensile strength of fiber strands for textile reinforcement structures. *Bauingenieur*(95), 325-334.
- Xu, S., & Li, H. (2007). Bond properties and experimental methods of textile reinforced concrete. *Journal of Wuhan University of Technology-Mater. Sci. Ed.*, 22(3), 529-532. <https://doi.org/10.1007/s11595-006-3529-9>